# Isolation of SRC in the $^3$He(e, e′pp)n$_{sp}$ Reaction Driven by One-Body Currents

K. Benslama, E.J. Brash, S. Dumalski, A. Fleck, G.M. Huber,
N. Knecht, G.J. Lolos, K. Papageorgiou, Z. Papandreou, A. Shinozaki
*Department of Physics, University of Regina, Regina SK S4S 0A2 Canada*

K. Aniol, M. Epstein, D. Margaziotis
*Department of Physics, California State University, Los Angeles CA 90032*

D. Meekins, R. Roche, A.J. Sarty
*Physics Department, Florida State University, Tallahassee FL 32306-4350*

R. Gilman, C. Glasshauser, G. Kumbartzki, R. Ransome, S. Strauch, X. Xiang
*Department of Physics, Rutgers University, Piscataway NJ 08855*

M. Kuss
*Thomas Jefferson National Accelerator Facility, Newport News, VA 23606*

J. Templon
*Department of Physics, University of Georgia, Athens, GA 30602*

P. Ulmer
*Department of Physics, Old Dominion University, Norfolk, VA 23529*

and the Hall A Collaboration

**This is a Hall A Collaboration Experiment.**

June 4, 1999

## Abstract

We propose a **surgical** measurement of short-range correlations (SRC), in inelastic electron scattering via the two proton knockout reaction $^3$He(e, e′pp)n$_{sp}$. Such correlations have a specific dynamical signature, in the ground state wavefunction of the target nucleus, which bridges the gap between nucleonic and quark degrees of freedom. As such, these measurements will provide severe constraints on existing theoretical models which employ realistic $N$-$N$ potentials, while at the same time providing the impetus for new calculations.

Our aim will be accomplished by separately measuring the longitudinal and transverse parts of the cross section, **for the first time,** as a function of dynamical observables, in an optimal kinemetical configuration. It is generally acknowledged that the $(e, e'pp)$ channel is an excellent candidate for probing SRC, however, the experiment must be designed carefully in order to minimize competing processes. This is best achieved by carrying out a Rosenbluth separation, in order to access the longitudinal part of the cross section, where the SRC signature is the cleanest and strongest. The optimal kinematical setting for such a measurement is that in which the two ejected protons are parallel and antiparallel, respectively, to the momentum transfer vector, and the energy transfer region of interest ranges from 500 to 900 MeV, with the **missing momentum of the neutron confined to spectator values.** The $^3$He nucleus has been selected because it is the lightest nuclear system for which the reaction can proceed, realistic wavefunctions are available, and a triple coincidence renders the experiment kinematically complete.

We propose to carry out these measurements using the two high resolution spectrometers in Hall A for detecting the scattered electron and the forward proton. The second proton, at backward angles, will be detected in either a magnetic or a scintillator-based, large solid angle proton detector. We request 436 hours of beamtime at a beam current of 35 $\mu$A.

# 1 Introduction

Electromagnetic probes are ideal for the study of the hadronic structure of nuclei and elementary particles. Indeed, electro- and photo-nuclear experiments have provided us with a wealth of information and have helped deepen our understanding of subnuclear degrees of freedom.

With the advent of high energy, high intensity electron accelerators operating with a continuous wave (CW) beam (nearly 100% d.f.), we are well poised to carry out many important and very interesting experiments in this field, especially in the transition region between intermediate energy and particle physics. Short Range Correlations (SRC) is one such topic which has recently generated much interest in the electromagnetic scientific community [1, 2, 3].

It is important to define the term SRC here, in the context of this proposal. We are referring specifically to the **short-range correlations driven by one-body nuclear currents.** These particular correlations correspond to an overlap of the quark bags of the individual nucleons at extremely small internucleon distances (ca. 0.5 fm); otherwise put, these correlations are associated with a process in the ground state wavefunction of the target nucleus that involves a **momentum exchange with zero energy exchange**. Basically, the two interacting nucleons simply exchange quarks, and this process cannot be described by traditional meson exchange, as evidenced by the difficulties that traditional boson exchange models have in describing the short-range character of the $N$-$N$ interaction. As such, SRC bridge the gap between nucleonic and quark degrees of freedom.

The aim of this experiment is to measure the longitudinal and transverse response functions in the $^3$He(e, e′pp)n$_{sp}$ reaction, as a function of dynamical quantities such as energy transfer and relative momentum between the two ejectile protons, among others. This approach will provide valuable (and severe) constraints to existing theoretical models (see Section 2.2).

In this proposal, we are not seeking to investigate traditional two-body correlations (2BC), such as meson exchange currents (MEC) or isobar currents (IC). These 2BC are relatively well understood, thanks to the wealth of data from pion and real-photon absorption, as well as the recent measurements at NIKHEF and elsewhere with virtual photons, and are subject of other experimental efforts at Jefferson Lab. Although the 2BC measurements themselves provide valuable cross-checks for the few-body calculations that may assist in the interpretation of the results of this experiment, here, **we have chosen kinematics so as to suppress 2BC and all other mechanisms competing with SRC.**

There are two approved experiments at Jefferson Lab with similar goals to ours (E89-031 and E97-106). Due to the specific methodology in each case, neither will access SRC in the direct manner employed here, but, nevertheless, they will provide valuable, complementary results that may assist in the theoretical deconvolution of the competing reaction mechanisms. The salient features of these two approved experiments, and their comparison to ours, are presented in Appendix A.

# 2 Correlations in Nuclei

## 2.1 Contributing Mechanisms

The successes of electro-nuclear scattering experiments, in terms of the resultant physics which has been extracted, are manifested in the simplicity and exactness of the electron-nucleon coupling mechanism. The *e-nucleon* and *e-nucleus* interactions are largely based on diagrams such as the one shown in Figure 1a, in which the energy and momentum of the exchanged virtual photon is transfered to a single nucleon, with the remaining (A-1) nucleons behaving as spectators. This mechanism is perturbative and allows the separation of effects due to the reaction mechanism from those due to nuclear structure, in the plane wave impulse approximation (PWIA) framework.

Even in deuterium, however, the need for other diagrams arose in order to account for the experimental data [4], such as IC like the $\Delta$ or $N^*$ resonances (Figure 1d) as well as non-resonant MEC (Figure 1e). Additionally, final state interactions (FSI) may become involved (Figure 1c). These FSI modify the four-momentum of the struck nucleon, thus altering the flux in any particular kinematical region, and complicate the interpretation of the results. The PWIA picture is not valid if FSI are large.

The existence of traditional 2BC (Figures 1d and 1e) has been firmly established in pion absorption measurements, spanning the last three decades. Recent real photon absorption results confirm this [5, 6]. It should be noted that pion- and real photo-absorption, at energies $\geq$ 100 MeV, probe primarily $N$-$N$ and $N$-$N$-$N$ correlations, due to the large momentum mismatch in these reactions. In addition, evidence for correlations has also been found via the $(e, e'p)$ reaction [7], in which the incoming virtual photon was interpreted to interact with a correlated nucleon pair. The characteristics of pions and real and virtual photons establish them as complimentary tools in the investigation of two-nucleon interactions. For a more detailed comparison of these probes, the reader is directed to reference [8].

However, **none of these approaches distinguishes or is able to separate SRC from 2BC** (Figure 1b from Figures 1d, e). Theoretically, a re-examination of $(e, e'p)$ and other data from Bates by Schiavilla [9], based on Coulomb sum rules and proton-proton correlations, has thus presented only *indirect* evidence for SRC, because of this inability to separate the different contributions.

## 2.2 Theoretical Issues

The information obtained so far on correlations from $(e, e'p)$ reactions has undoubtedly been instructive in many ways, but has not provided an unambiguous signature of SRC, free from competing mechanisms. To achieve this, we need to study the $(e, e'pp)$ channel, which is the best candidate for two-proton ejection investigations, provided that the two detected protons are those which were initially correlated in

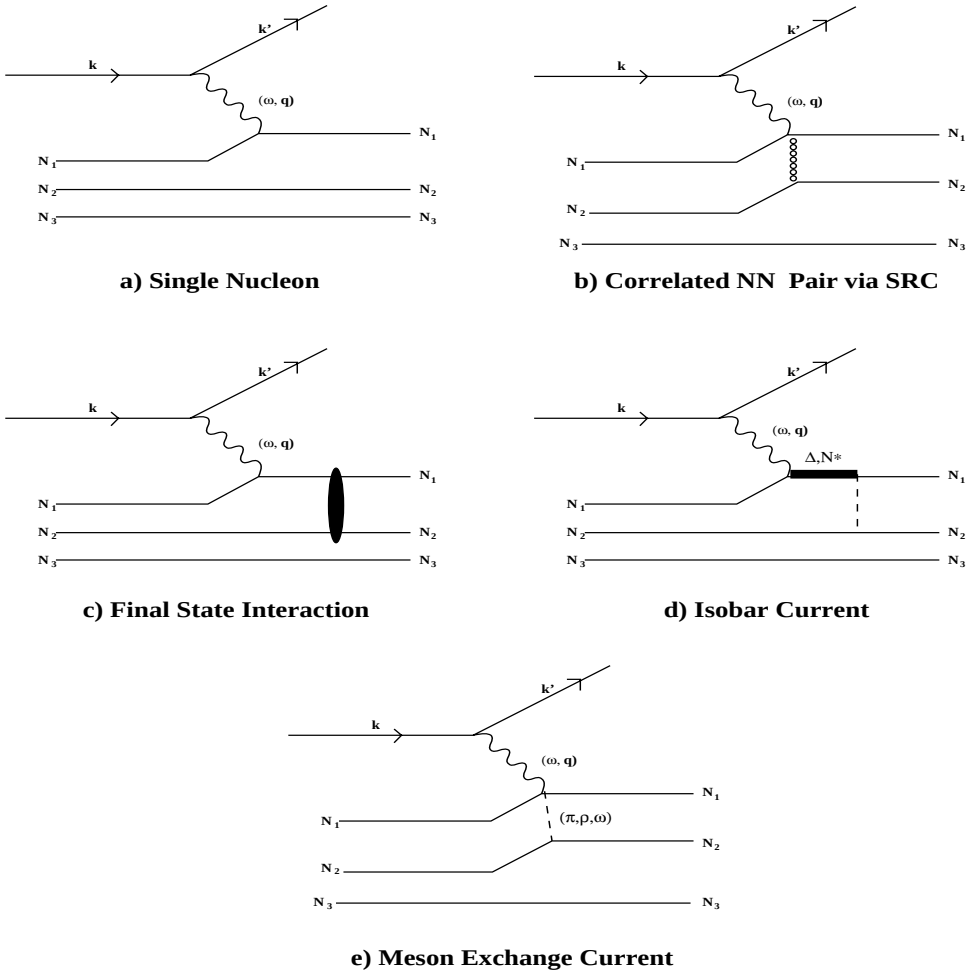


Figure 1: Diagrams contributing to the $^3$He(e, e′pp)n channel.

the ground state of the nucleus [10, 11]. This statement will be substantiated below.

As mentioned in the introduction, SRC bridge the gap from traditional to quark degrees of freedom. Even though the following theoretical discussion, which is based on nucleonic and mesonic degrees of freedom, is not a sufficient description of SRC at all internucleon distances, it nevertheless is applicable to the lowest $\omega$-$q$ region of this proposal; i.e. it provides a framework for the interpretation of the data from "one side of the bridge". On the other hand, reliable theoretical calculations do not exist for the higher $\omega$-$q$ regime, nor do experimental measurements; it is hoped that the results extracted from this experiment will provide the impetus to theorists to develop an approach from the "other side of the bridge."

In nuclear reactions, where two nucleons are emitted, information on the two-hole spectral density function and the two-body density matrix [11, 12, 13] can be obtained. From such investigations one hopes to extract the two-body density in the ground state of the target nucleus. One popular approach, in this pursuit, has been to employ correlation or defect functions [11, 14, 15]. These functions may be

of a central, spin-spin or even tensor form. The various models differ in their choice of correlation function (soft- or hard-core), with a direct effect on the magnitude of the cross section (e.g. [13]). In other models, the same effects are implicitly built into the formalism [10].

As mentioned above, at the quark level, SRC manifest themselves as overlap of the quark-filled bags. Theoretical calculations, based on nucleonic degrees of freedom, do not look at things this way. The leading groups who calculate $(e, e'pp)$ cross-sections assemble a number of ideas. The interaction with the virtual photon is well-understood, and more importantly MEC, IC, and FSI are treated completely, by solving the scattering theory problem exactly. However, while the target spectral function is calculated in an exact manner, at the heart of it is an $N$-$N$ potential that is phenomenological and based on meson exchange. As such, the short-range character of the interaction is implicitly built into the $N$-$N$ potential and cannot be decoupled. As an illustration, though, we point to a recent comparison of theoretical models based on realistic $N$-$N$ potentials to $^4$He(e, e'p)$^3$H data [16]. In this paper, the authors show that at high missing recoil momentum, the $N$-$N$ potentials which are known to describe short-range behavior well, fare better in the description of the data.

Clearly, although the effect of SRC is not accounted for in an identical prescription within the different theoretical approaches, this is not a concern for the work proposed here since we aim to isolate the reaction mechanism of Figure 1b **experimentally.** This is exactly where the strength of the proposed experiment lies: not only will the magnitude of the longitudinal and transverse cross sections be measured accurately, but their dependence on dynamical variables will be extracted and serve as a vital ingredient in discriminating between the various models.

In the $(e, e'NN)$ reaction, one can describe the measured differential cross section in terms of structure functions, which represent the response of the nucleus to the longitudinal and transverse components of the virtual photon in the interaction. These structure functions depend only on the kinematical quantities $\omega$, $\vec{q}$ and the angles between the momentum transfer $\vec{q}$ and the individual particle momenta $\vec{p}'$ of the two emitted nucleons [13]. The transition matrix element in these functions consists of the one- and two-body parts of the current operator, $J^{(1)}$ and $J^{(2)}$, respectively:

$$J^{\mu}(\vec{r}, \vec{r}_1, \vec{r}_2) = J^{(1)\mu}(\vec{r}, \vec{r}_1) + J^{(1)\mu}(\vec{r}, \vec{r}_2) + J^{(2)\mu}(\vec{r}, \vec{r}_1, \vec{r}_2) \qquad (1)$$

where $\vec{r}$, $\vec{r}_1$, $\vec{r}_2$ are the coordinates of the recoiling nucleus and the two ejected nucleons, respectively.

Due to their nature, the two-body current operators, $J^{(2)}$, include MEC and IC terms and thus eject two nucleons that are correlated via 2BC. On the other hand, the one-body operators, $J^{(1)}$, which dominate in the longitudinal channel, can contribute to two-nucleon emission **only** via SRC. As such, it is **the one-body operators in the $(e, e'pp)$ channel which are behind the motivation of this proposal.**

## 2.3 Suppression of IC

It is generally accepted that SRC, driven by one-body currents, are linked to the longitudinal component of the *e-nucleus* cross section. Thus, whereas the $J^{(2)}$ currents are required for the description of $(e, e'pn)$ and $(\gamma, pp)$ reactions [13] that are predominantly transverse, the $J^{(1)}$ currents exclusively probe the longitudinal structure function of the reaction. This feature follows the fact that, in contrast to the $(e, e'pn)$ channel, the transverse cross section in the $(e, e'pp)$ reaction is strongly suppressed due to three reasons [10, 11]:

- the $pp$ pair has no dipole moments for the virtual photon to couple to;
- The meson in-flight terms of MEC currents do not contribute here (to first order); and
- the formation of the intermediate $\Delta$ is suppressed, as the dominant $J^\pi = 1^+ p\Delta^+$ state can not decay in the $pp$ channel.

These restrictions, on one hand, result in a small cross section for the $(e, e'pp)$ process, but on the other hand the SRC component in the nuclear wavefunction, obscured otherwise, becomes accessible.

A strong endorsement for the above argument is provided by the TAGX results shown in the right panels of Figure 2 [5, 6]. The upper panel of these displays $^3$He$(\gamma, \mathrm{pp})\mathrm{n_{sp}}$ events associated with a spectator neutron (missing momentum consistent with Fermi motion), labelled as 2N(pp) – two-nucleon absorption. The lower panel, in contrast, contains the $^3$He$(\gamma, \mathrm{pp})$n events associated with a neutron which participates in the energy and momentum sharing, following three-body phase space with a constant matrix element, and is appropriately labelled as 3N (three-nucleon absorption of the photon). A missing mass restriction assured the elimination of pion production events from both these channels in the analysis.

The transverse $\Delta_{1232}$ resonance is manifest in the lower-right panel, as well as in the $^3$He$(\gamma, \mathrm{pn})$p reaction with explicit detection of the neutron and with a spectator proton [5], but is notably absent from the 2N(pp) panel. This is an unambiguous indication that the $pp$ channel is inherently free of transverse admixtures, even in this extreme case of a purely transverse probe! This is obviously also the case for the transverse components of higher lying $\Delta$ and $N^*$ resonances which decay into two nucleons in this photon energy region. Furthermore, analysis of recent $^3$He$(\gamma, \mathrm{pp})\mathrm{n_{sp}}$ TAGX data, at photon energies up to 1.1 GeV, has revealed complete absence of any resonant benavior in the total cross sections [17].

It is evidently clear that the choice of the $^3$He$(\mathrm{e}, \mathrm{e'pp})\mathrm{n_{sp}}$ channel (with a cut on the missing mass to exclude pion production) naturally eliminates the $\pi N$ and $\pi\pi N$ decay channels of these resonances. Moreover, the coplanarity built into this experiment favors the acceptance of the $(e, e'pp)$ SRC channel over that of any resonant decay channels, which tend to populate the phase space over $4\pi$, a fact verified by Monte Carlo simulations that we have carried out. This was also a contributing factor in the $(\gamma, pp)$ results from TAGX [6].

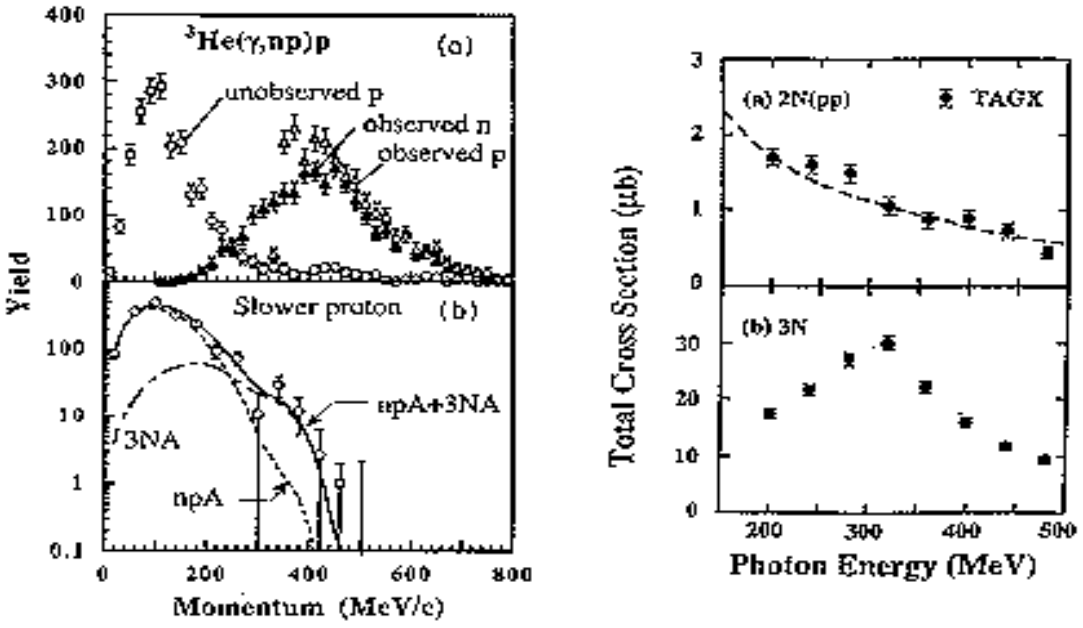


Figure 2: *Left panels:* Momentum spectrum (a) of the observed neutrons (solid triangles) and protons (open triangles), and unobserved protons (open circles) from the $^3\mathrm{He}(\gamma, \mathrm{np})\mathrm{p_{sp}}$ reaction over the entire $E_\gamma$ range, and (b) of the slower proton among observed and unobserved protons at $E_\gamma = 245 \pm 80\, MeV$.
*Right panels:* Total cross-sections as a function of incident tagged photon energy for (a) two-body absorption leading to a *pp* final state and (b) for the three-body absorption leading to *ppn* final state in the $^3\mathrm{He}(\gamma, \mathrm{pp})$ reaction from reference [6]. The dashed line in (a) is from reference [19], for photo-absorption on a *pp* bound pair assuming $E2$ transition and *pn*-like radial wavefunction.

To reiterate, we note again the advantage of the $^3\mathrm{He}(\mathrm{e}, \mathrm{e'pp})\mathrm{n_{sp}}$ channel for the pursuit of SRC: **the transverse $\Delta_{1232}$ and other higher lying resonances do not contribute to this channel**, effectively eliminating diagram 1d. Furthermore, the unobserved neutron must conform to a spectator momentum, as illustrated in the upper left panel of Figure 2, in order to to suppress the participation of all three nucleons in the reaction. This is ensured by requiring that **the missing momentum in the reaction be consistent with that of Fermi momentum of a single nucleon in $^3$He.** This last point is supported by theoretical calculations, as explained in the Section 4.

## 2.4 Effects of FSI

The question of FSI (Figure 1c), and the associated modification of physics observables, is an issue for consideration. We assert that FSI comprise a small component in the $^3\mathrm{He}(\mathrm{e}, \mathrm{e'pp})\mathrm{n}$ channel. In addition, the selection of kinematics with one proton

parallel to $\vec{q}$ and the other antiparallel, contributes further to the suppression of this competing mechanism [18], even when compared in magnitude to the small SRC longitudinal cross section. Evidence for this is supplied below. Here, and in the ensuing discussion, we are referring exclusively to "hard" ($N$-$N$ scattering) FSI. "Soft" FSI, on the other hand, have the two nucleons travelling parallel to each other, and are completely eliminated in back-to-back kinematics. Nevertheless, (hard) FSI calculations will need to be applied towards the interpretation of the data, and such calculations are reasonably advanced and reliable, over the entire dynamic range of this experiment.

The assertion of diminished FSI is strongly supported by the expectation that these processes are much smaller in $^3$He than in large nuclei, and by data from TAGX on $^3$He$(\gamma, \mathrm{NN})$p and $^3$He$(\gamma, \mathrm{pp})$n [5, 6], which show very little evidence for FSI modifying the momentum distribution of the unobserved nucleon, as can be seen in Figure 2. The absence of any significant high momentum components in the left panel (b) of this figure is interpreted as lack of FSI, as the data can be described well by the sum of the $npA$ (two-nucleon absorption) and $3NA$ mechanisms alone. Moreover, if FSI were "leaking" into the $pp$ channel (even at the 4% level), one would expect the shape in the upper right panel to be similar to that in the lower right panel, since the cross section in the latter is ten times larger. Similar conclusions have been reached in pion absorption experiments on $^3$He [20, 21]. Indeed, in the latter of these references, the **summed** contribution of FSI **and** $\pi$-$N$ initial state interactions to the reaction cross section was a mere 6% [21]. Numerous other pion absorption experiments have shown that FSI begin to become problematic for more complex nuclei such as $^{12}$C (e.g. [22]).

On the theoretical front, "exact" calculations on $^3$He support the argument that the FSI contribution is small [23]. These calculations employ the Faddeev method for calculating the ground state and continuum wavefunctions of $^3$He, and apply relativistic kinematics for the outgoing nucleons. In the kinematical domain of this proposal, the FSI contribution for the $^3$He$(\mathrm{e}, \mathrm{e'pp})$n reaction is on the level of 10% over all phase space. It follows that in the longitudinal and spectator-neutron part of the phase space, specifically, the FSI contribution is expected to be negligible [18].

More recent calculations on the $A = 3$ system have made a significant step forward in the treatment of FSI [24]. Specifically, the full calculations of $ppn$ breakup from $^3$He using realistic $N$-$N$ forces with full inclusion of all rescattering processes, and including all relevant $N$-$N$ force components, have been carried out. This procedure, which employs the solution of Faddeev-like integral equations, can be used to check the role of FSI via theoretical calculations. Depending on the kinematical conditions, a significant deviation from PWIA may be observed, but at least now a reliable theoretical treatment of FSI is possible at energy transfers below 500 MeV. The general trend is that FSI are diminished in importance, as the momentum transfer increases. In addition, the back-to-back (with respect to $\vec{q}$) nature of super-parallel kinematics, severely suppresses $NN \rightarrow N'N'$ quasi-free scattering, which constitutes the bulk of FSI, as this process peaks at 90° in the center of mass. Additional

suppresion factors arise from restrictions on the missing momentum, missing energy, and the coplanarity between the three-momenta of the two ejected protons with respect to the momentum transfer vector, i.e. on the quantity $\vec{q} \cdot (\vec{p}_{p_1} \times \vec{p}_{p_2})$.

Finally, theoretical $N$-$N$ and $\pi$-$N$ calculations are quite advanced. Indeed, accurate $N$-$N$ forces exist up to nucleon kinetic energies exceeding 1 GeV, and the Glauber method is used reliably to calculate FSI even above 1 GeV [25]. All these considerations justify the large values of $q$ and the choice of kinematics selected for this work.

In summary, we contend that the $^3$He(e, e′pp)n$_{\rm sp}$ cross section does not contain significant FSI, as evidenced by experimental measurements with real photons and pions. The back-to-back kinematics, the L/T separation, and cuts in the offline analysis further enhance the SRC component over that of FSI, as will be discussed in Sections 3 and 4. What remains of FSI can then be modelled by any of the groups active in this field (e.g. [23, 24, 25]).

## 2.5 The Role of MEC

Traditional, non-resonant MEC diagrams involve the exchange of $\pi$, $\rho^0$ and $\omega$ mesons (see Figure 1e). References in the literature (e.g. [10]) claim that the meson in-flight terms of MEC altogether are suppressed in the *pp* channel. For the remaining terms, the L/T separation will separate the transverse components of these exchange particles from the SRC contribution, as mentioned in Section 2.3. Theoretically, it is not known whether these exchanges involve a longitudinal component, let alone how large it is. In any case, reliable, Faddeev-type calculations exist for $^3$He, and the nature of $\pi$-$N$ and $\rho^0$-$N$ coupling is understood well enough to allow the determination of the longitudinal contributions of these processes. Finally, as far as the $\rho^0$-$N$ and $\omega$-$N$ interactions are concerned – which are important ingredients at short distances – recent and proposed measurements on $\rho^0$ photoproduction in a number of different nuclei [26, 27], will quantify the observed nuclear medium modifications of the masses and coupling constants of the $\rho^0$ and $\omega$, and thus may lead to improved $\rho^0$-$N$, $\omega$-$N$, and in turn $N$-$N$ amplitudes in nuclei.

## 2.6 Summary of Contributing Reaction Mechanisms

- Our aim is to isolate the SRC reaction mechanism (Figure 1b).
- The quasi-free mechanism (Figure 1a) is excluded, due to the coincident detection of both protons and the scattered electron.
- FSI (Figure 1c) are strongly suppressed, due to the choice reaction channel, target, kinematics, and analysis techniques.
- The IC channels (Figure 1d) are essentially eliminated, again due to the choice of the $(e, e'pp)n_{sp}$ channel, the L/T separation, exclusion of pion production,

and the coplanarity of the reaction.

- MEC currents (Figure 1e) are suppressed for similar reasons to IC, and are theoretically calculable.

**The proposed measurement will be conducted in the $^3$He$(e,e'pp)n_{sp}$ channel. An L/T separation will be carried out, in super-parallel kinematics and at three values of $\omega$. These conditions render the experiment as the ONLY experiment, proposed at Jefferson Lab so far which can directly access the small SRC component in the reaction. All other efforts will provide useful, complementary information on this subject, but are not designed to isolate SRC.**

In the subsequent section, we summarize the state-of-the-art $(e,e'pp)$ channel measurements from NIKHEF, and apply the knowledge obtained to the choice of kinematics in Section 4.

# 3 SRC Evidence from $^3$He,$^{16}$ O(e, e′pp)n

The first topical results from the medium-energy CW accelerators at NIKHEF, Mainz, and Bates on a variety of nuclei, have provided significant data on correlations in nuclei. As examples, we mention the experiments which studied the exclusive $^2H(e,e'p)$ at large missing momenta [28], as well as the semi-exclusive $^{12}$C(e, e′p) reaction [29]. The difficulties experienced in separating the various competing reaction mechanisms is a fact admitted by the authors of these papers, and they concluded that the most effective technique for enhancing the contribution of SRC is to study the two-proton emission channel, $(e,e'pp)$. Indeed, this has been the path that has been followed, as described in references [30, 31, 32, 33].

We begin the review of the recent NIKHEF $^3$He(e, e′pp)n experiments by examining the missing momentum of the residual (A-2)-system, $p_m$. This is an important parameter in tuning the kinematics towards promoting the SRC component. In Figure 3, we show the differential cross-section for the $^3$He(e, e′pp)n reaction at $\omega = 220$ MeV and $q = 305$ MeV/c as a function of the missing momentum of the neutron [33, 34]. The continuum Faddeev calculation, which does **not** include any two-body hadronic currents, tends towards the data at low $p_m$, but significantly underestimates the data at high missing momentum. This is not surprising, since large $p_m$ signifies an "active" (non-spectator) third nucleon, which is consistent with processes such as 2BC, FSI, and three-nucleon absorption. We conclude here that SRC can be reliable extracted only under the condition that $p_m$ is consistent with Fermi momentum of the third nucleon on $^3$He, as already discussed in Section 2.3.

In Figure 4, we show differential cross-section results for the $^{16}$O(e, e′pp) reaction for three values of $\omega$, and a single value of $q = 305$ MeV/c [33, 35]. The upper panels correspond to the ground state of the residual nucleus, while the lower panels to the lowest $2^+$ excited state of $^{14}$C. There are a number of important features to point out.

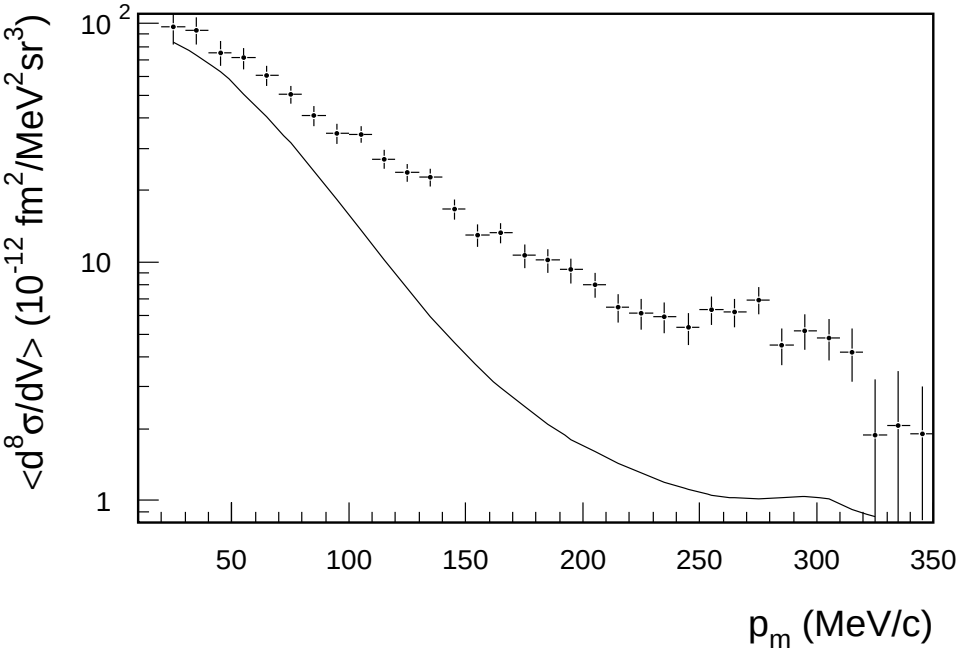


Figure 3: Cross-Section for the $^3$He(e, e′pp)n reaction from NIKHEF. The curve represents the results of a continuum Faddeev calculation, from reference [24].

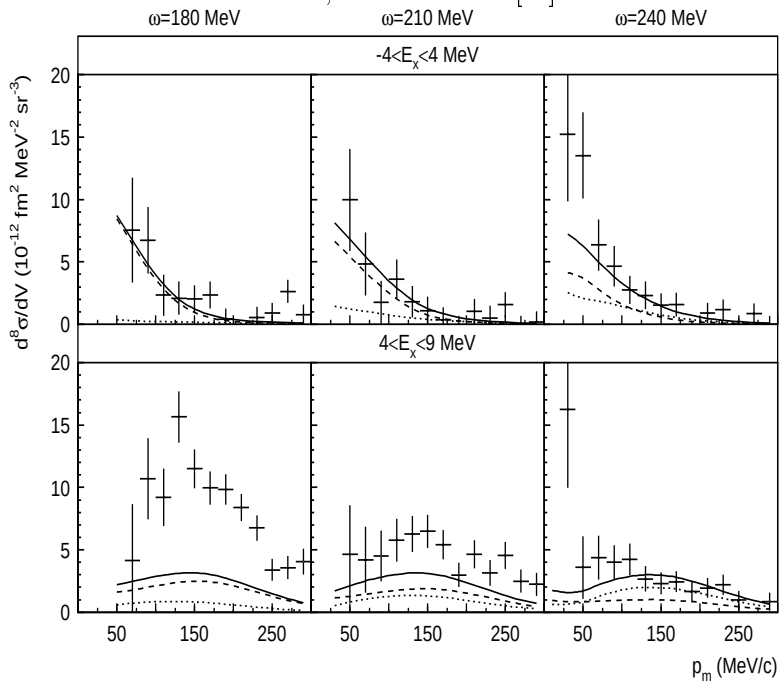


Figure 4: Cross-Section for the $^{16}$O(e, e′pp) reaction from NIKHEF. The solid curves represent calculations of the Pavia group [36], with the dashed (dotted) curves indicating the contribution of the one- (two-) body hadronic current.

First, we note that the agreement with the full theoretical calculations of the Pavia group, which includes SRC as well as traditional 2BC processes, is striking for the ground state scattering. This fact gives further credence to the claim that focusing on an exclusive channel, where the quantum numbers of the residual system are explicitely known, is most effective. Second, the contribution of the 2BC processes increases with increasing $\omega$. Finally, we note that the signature for SRC here is the specific $L = 0$ dependence in the cross-section, suggesting the dominant role for the knockout of a pair of nucleons in a relative S-state, driven by SRC.

While these results from NIKHEF are impressive, their authors note two specific issues of concern. The first is that one can see already in the $\omega = 240$ MeV region the increasing importance of $\Delta$ contributions as one approaches this resonance (dotted lines in the upper three panels of Figure 4). This is in contradiction to the TAGX results with real photons on $^3$He. Considering the straightforward, model-independent TAGX analysis, we believe that the $^3\mathrm{He}(\mathrm{e},\mathrm{e'pp})\mathrm{n_{sp}}$ channel is relatively free of a $\Delta$ admixture. The second is that no L/T separation was performed at NIKHEF. Such a separation would allow one to **uniquely** determine the longitudinal structure function, implying that any measured strength would be completely due to SRC-driven processes, and as a result the interpretation of the data is much less model-dependent.

Based on this most recent evidence, we ascertain that only a kinematically complete experiment in the $(e, e'pp)$ channel, which combines the features of a L/T separation based on the exchanged virtual photon, super-parallel kinematics, large relative momentum between the two outgoing protons, and small missing momentum of the residual system, has the ability to **directly** access SRC. These critical requirements, together with the expected small SRC cross section, dictate the need for discrete detectors probing specific regions of phase space at a high luminosity.

# 4 The Experiment

The crucial aspects of our experiment are itemized below.

## 4.1 Rosenbluth Separation in the $(e, e'pp)$ Channel

The $(e, e'pp)$ reaction is the best tool for investigating SRC, as explained above, as long as one can minimize the transverse and interference components of the nuclear response. By confining the ejectiles in-plane (**coplanar**) with $\vec{q}$, and in back-to-back (**super-parallel**) kinematics, only the longitudinal and the transverse structure functions survive [10, 11, 37]. Super-parallel kinematics are defined here as the kinematics where one proton has its momentum vector parallel to $\vec{q}$, while the other proton is ejected anti-parallel to $\vec{q}$. However, since even at forward angles the transverse component may still contribute, a proper **L/T separation** must be performed to decouple the longitudinal cross section.

## 4.2 The Choice of Energy Transfer Region

There are a number of factors underlying the optimal choice of the $\omega$ region for this experiment, as explained below.

At the quasi-elastic region, SRC investigations in the $(e, e'pp)$ channel are hindered by the fact that the energy and momentum transfers are small. This results in small relative momentum between the two ejected protons, and a very low momentum of the proton at backward angles. The first diminishes the effect of SRC, since these are coupled to high relative momenta, and the second renders the detection of the backward proton impossible due to detector threshold effects.

In the "dip" region (between the quasi-elastic peak and the $\Delta$ resonance), the experimental data clearly indicate more strength than the basic $e$-$p$ interaction can account for. The magnitude of the missing strength in this region varies among different models, and some can account for this strength, provided that several mechanisms are taken into consideration [38]. In the transverse sector of this region, the $\Delta$ resonance is one of the dominant contributors. Neverthess, this is not a concern for this proposal, since the method employed to here isolate SRC is largely impervious to IC contributions, as explained in Section 2.3. A similar argument holds for the region of higher $\Delta$ and $N^*$ resonances.

Having said this, the lower bound on the $\omega$ region arises from two experimental requirements: a) the second (backward) proton must have sufficient energy to exit the target and register a hit in the backward detector with a momentum distribution well into the "flat" detector acceptance region (see Section 4.4 and Appendix A); and b) an adequate lever arm for the proposed L/T separation is required. With a threshold of 45 MeV for the second proton, and a desired $\epsilon$ lever arm of at least 0.4, the lowest feasible value is $\omega = 500$ MeV.

From the upper-right panel of Figure 2, we observe that the total $^3$He$(\gamma, \mathrm{pp})\mathrm{n_{sp}}$ cross section is decreasing as a function of photon energy. The TAGX collaboration, in a separate analysis [17], has measured this cross section to 1.1 GeV photon energy. At this value, the cross section becomes exceedingly small, and the associated beamtime unfeasible. Thus, we assume $\omega = 900$ MeV for our upper bound. It is worthwhile mentioning, that at this energy transfer, even the transverse component from the L/T separation is of theoretical interest [39], as no measurements exist. Moreover, values of three-momentum transfer much above 1 GeV/c lead to an increased ratio of the longitudinal to the transverse cross section, at the expense, however, of substantially decreased strength.

In summary, the region of $500 \leq \omega \leq 900$ MeV is the most promising for this proposal, based on the experimental feasibility issues. Close to 500 MeV, reliable calculations exist [14, 24]. At higher values of $\omega$ only reliable $N$-$N$ models exist (e.g. [25]), and we hope that the new data provided from this experiment will constrain existing models [10], and will also encourage other groups to pursue models based on quark degrees of freedom.

## 4.3 The Target Nucleus ($^3$He)

The nature of SRC dictates a target of high nuclear matter density, but low $A$. The latter requirement stems from pion absorption results from TRIUMF and LAMPF, which indicated that heavier nuclei complicate the picture since they suffer from increased FSI complications.

In addition, since the SRC cross sections are expected to be small, any uncertainties in the angular correlations and missing four momentum information will complicate the analysis, perhaps even to the point of loss of information. We thus require a **kinematically complete experiment**, at least in the first step on the road to understanding SRC. This will allow us to restrict our measurements to regions of phase space where the momentum distribution of the neutron is consistent with a spectator (Fermi) momentum, in order to ensure that the energy and momentum transfer in the reaction were entirely absorbed by the two-proton cluster. Clearly, one has to resort to a triple-arm experiment on $^3$He to achieve all this. In fact, the $^3$He(e, e′pp)n reaction is not only kinematically complete, it is over-constrained.

Theoretically, $^3$He is a very attractive target: it has well described ground state and continuum wavefunctions, and the electrodisintegration of $^3$He can be treated fully by solving Faddeev-like integral equations, using realistic $N$-$N$ forces [24]. The inter-nucleon distance in $^3$He is not that much different than heavier nuclei and thus the SRC signatures should be strong enough to manifest themselves.

The choice of $^3$He as a target has received the strong endorsement of J.M. Laget, J.A. Tjon, W. Glöckle, J. Ryckebusch and R. Schiavilla, in our private communications with them. We consider that the ("tuna-can") target to be used in this experiment will be a standard facility at Hall A by the time this experiment runs.

We mention here that although valuable insights have been obtained from the $^{12}$C(e, e′pp) and $^{16}$O(e, e′pp) experiments at NIKHEF and Mainz, their deconvolution relies heavily on theoretical calculations. Several of these are becoming state-of-the-art efforts. However, we assert that the interpretation our $^3$He(e, e′pp)$n_{sp}$ proposed experimental results will be the least model-dependent, due to outright suppression of competing reaction mechanisms. **The $^3$He(e, e′pp)$n_{sp}$ channel proposed here will provide the cleanest SRC signature among all similar efforts.**

## 4.4 The Detectors

The electron and forward going proton will be detected in the $HRSE$ and $HRSH$ Hall A spectrometers, respectively. These devices will be operated in their standard configuration.

The statistical requirements, due to the low cross sections, demand an experiment with high luminosity and the use of discrete detectors, which can handle the instantaneous counting rates. The issue of sustainable count rates is being tackled by the Hall A Third Arm working group, and their findings will dictate the precise

requirements (including shielding) of the third arm.

Nevertheless, simply as reference for the arguments below on the expected beamtime for this experiment, we cite the HADRON3 detector used in experiments at NIKHEF [40]. This device consists of 128 scintillators which provide segmentation in all three dimensions, and is well suited to accommodate large instantaneous counting rates. At a nominal distance of 80 cm from the target, this device subtends solid and opening angles of 220 msr and 27° (segmented in 1.1° slices), respectively, and has been proven to handle a luminosity of $10^{37}$ cm$^{-2}$s$^{-1}$ on a $^3$He target at an angle of 140° with respect to the beam, and at a beam energy of 560 MeV, by using a 1 mm Fe absorber at its entrance.

The tolerated luminosity can be increased substantially by increasing the absorber thickness to 2-3 mm, without significantly degrading the energy resolution and detection threshold. Furthermore, the device will be placed at larger distances from the target, as explained below, which reduces the intercepted singles rate. The accompanying reduction in solid angle is not a concern, since only the center portion of the detector is needed in our L/T separation. Finally, the second proton in our experiment is always emitted at angles $\geq 140°$ (see table below), where the background is expected to be under control. The point being made here is that **any** such plastic scintillator detector should be able to tolerate luminosities of the order of $4\times10^{37}$ cm$^{-2}$s$^{-1}$, once adequate shielding has been employed.

Recently, we have examined the possibility of using the Big Bite spectrometer as the third arm in this experiment [41]. This device subtends a 100 msr solid angle and accepts momenta between 300-900 MeV/c, values that are compatible with this experiment, with the added advantage of lower susceptibility to background. The rates with this device may be more favorable than those based on HADRON3, an effect largely dependent on the background suppresion achievable. The counting rates presented in the subsequent section reflect the most conservative scenario of using HADRON3.

## 4.5 Kinematics and Beamtime Request

We have chosen kinematic geometries in regions of phase space where the cross sections are as large as possible, while the description of the knock-out process is simplified. Restrictions on the kinematics also arise from the L/T lever arm, detector thresholds and the fact that the detectors must not physically overlap, as well as from the desired energy transfer region and the suppression of competing reactions (MEC/IC/FSI), explained previously.

We propose L/T measurements at three values of $\omega$. This will permit the extraction of the energy dependence of the longitudinal component, a feature highly desirable for any theoretical description of SRC. It should be noted that photo-absorption experiments have established that the cross section for two-nucleon absorption on a T=1 *pp* pair drops rapidly with photon energy (see Figure 2). This reaction is dominated by 2BC $N$-$N$ correlations. Incidentally, the *pn* cross section also drops

with energy past the $\Delta$, which implies that FSI and rescattering also decrease with energy. Moreover, the $\omega$ dependence will prove useful in the separation of any residual competing channels which may survive the aforementioned suppression methods and the analysis cuts (see Section 2). E.g., the FSI ($N$-$N$ based) energy dependence is known and can be be fit to the data in a multi-parameter analysis.

The proposed kinematics are listed in Table 1, with both forward and backward kinematics indicated for each point. The $\omega$ = 500 MeV point is near the upper end of validity of the theoretical codes which make reliable calculations [14, 24], with the exception of FSI calculations which rely on standard $N$-$N$ or Glauber type calculations [25], and which are valid up to and past 1 GeV. The cross sections here turn out to be high enough that these measurements can be achieved in a few hundred hours at a luminosity of $4\times10^{37}$ cm$^{-2}$s$^{-1}$, given the detector acceptances in Table 2.

Table 1: Kinematics for the Proposed Experiment

| $Q^2$ $GeV/c^2$ | $E_e$ $MeV$ | $\omega$ $MeV$ | q $MeV/c$ | $\theta_e$ (deg) | $\theta_p$ (deg) | $\epsilon$ | $p_{p1}$ $MeV/c$ | $p_{p2}$ $MeV/c$ |
|---|---|---|---|---|---|---|---|---|
| .250 | 2445 | 500 | 708 | 13.2 | -38.8 | .949 | 1020 | 312 |
| | 1045 | | | 38.7 | -28.8 | .670 | | |
| .350 | 2445 | 700 | 917 | 16.5 | -32.7 | .909 | 1264 | 347 |
| | 1245 | | | 42.1 | -23.5 | .585 | | |
| .400 | 3245 | 900 | 1100 | 13.2 | -29.1 | .925 | 1488 | 388 |
| | 1445 | | | 41.7 | -19.3 | .532 | | |

Our count rate estimates are based on a PWIA model (modified MCEEP MC simulation) which agrees with the predictions of reference [24]. Furthermore, a comparison of the MCEEP results to the calculations of Laget [39] is shown in Table 3, which demonstrates that even at $\omega$ = 900 MeV the agreement is reasonable for both forward and backward measurements. Calculations by another group [42] agree quantitatively, as well. The details of our calculations are presented in Appendix A.

The count rates for the full acceptance of the spectrometers are shown in Table 4,

Table 2: Detector Acceptances

| HRSE | HRSH | Hadron3 |
|---|---|---|
| $\Delta p/p$=$\pm$5.0% | $\Delta p/p$=$\pm$5.0% | $T_p^{min}$=45 MeV |
| $\Delta\Omega$=6.7 msr | $\Delta\Omega$=6.7 msr | $\Delta\Omega$=40 msr |
| $\Delta\theta$=$\pm$30 mr | $\Delta\theta$=$\pm$30 mr | $\Delta\theta$=$\pm$116 mr |
| $\Delta\phi$=$\pm$65 mr | $\Delta\phi$=$\pm$65 mr | $\Delta\phi$=$\pm$116 mr |

Table 3: MCEEP PWIA and Laget Cross Sections for Super-Parallel Kinematics

| L/T | $\omega$ MeV | q MeV/c | MCEEP units* | Laget units* | Ratio $\sigma_{MCEEP}/\sigma_{Laget}$ |
|---|---|---|---|---|---|
| Forward | 900 | 1076 | $1.17\times10^{-11}$ | $1.53\times10^{-11}$ | 0.76 |
| Backward | | | $1.73\times10^{-12}$ | $1.40\times10^{-12}$ | 1.24 |
| *units=$fm^2/(MeV/c)(MeV)sr^3$ | | | | | |

Table 4: Count Rate Estimates for Super-Parallel Kinematics

| $E_e$ MeV | $\omega$ MeV | q MeV/c | $\theta_e$ (deg) | Count Rate $hr^{-1}$ | Acceptance Matched $hr^{-1}$ | Time (hrs) |
|---|---|---|---|---|---|---|
| 2445 | 500 | 708 | 13.2 | 7543 | 1876 | 5 |
| 1045 | | | 38.7 | 398 | 398 | 25 |
| 2445 | 700 | 917 | 16.5 | 1681 | 468 | 21 |
| 1245 | | | 42.1 | 102 | 102 | 98 |
| 3245 | 900 | 1100 | 13.2 | 1190 | 321 | 31 |
| 1445 | | | 41.7 | 39 | 39 | 256 |
| Total requested beamtime | | | | | | 436 |

where we have assumed a target density of 930 mg/cm$^2$ (as in E89-044) and a beam current of 35 $\mu$A, leading to a luminosity of $4\times10^{37}$ cm$^{-2}$s$^{-1}$. In the second to last column of this table, we show the acceptance matched rates. In the final column, we show the beam time required to obtain 5000 counts at each kinematic setting. We have estimated the efficiency of the various cuts on the data (missing momentum - spectator neutron, missing mass - no pion produced, coplanarity) to have an efficiency of 0.10-0.20, leading to a 3-5% statistical uncertainty, which translates into an error of 5.8% in the longitudinal and 5.4% in the transverse response functions.

We feel it is important to mention the anticipated precision of our measurement based on currently available theoretical predictions and our understanding of the systematic uncertainties of cross section measurements in Hall A. At the low $\omega$ kinematics of this experiment, where we expect the existing theoretical models to have higher confidence, the SRC contribution to the longitudinal component of the cross section lies between 50-90% of the total strength, dependent on the precise kinematics [24, 36, 42]. In the higher $\omega$ kinematics, calculations indicate an even greater dominance of the longitudinal component [39]. Given the $\epsilon$ lever arm from the table, and assuming a total systematic uncertainty of 5%, we expect to be able to measure the longitudinal component to less than 10% of its value.

# 5 Summary Justification

In a direct manner, SRC probe quark degrees of freedom in the nuclear wavefunction. As far as the physics goals addressed in this proposal are concerned, we will focus on a precision measurement in a specific region of phase space, in order to determine the exact nature of SRC and their contribution to the ground state nuclear wavefunction, and in specific kinematics which allow the measurement of large values of the relative momentum. These correlations can be only accessed directly via a L/T separation on the $^3$He(e, e′pp)n$_{\rm sp}$ channel which will isolate the one-body current reaction mechanism, and will provide constraints to theoretical calculations. We expect a 3-5% statistical accuracy, while systematic uncertainties are expected to be around 5%. The key features of the experiment are summarized below.

## Surgical Approach

1. *Reaction Channel:* The optimal channel for this study is $(e, e'pp)n_{sp}$, which leads to a suppression of the competing IC, FSI and MEC reaction mechanisms.

2. *Rosenbluth Separation:* Measurements must be made with adequate kinematical constraints to supress any MEC and IC contributions which "leak" into the *pp* channel. This requires a L/T separation with an adequate lever arm, and the experiment must be able to handle high luminosities. Discrete detectors (with a good $S/N$ ratio) are best suited to such conditions.

3. *The Kinematics:* In order to further minimize FSI we will detect the two outgoing protons parallel and anti-parallel to the momentum transfer vector, while ensuring a large relative momentum between the two ejectile protons.

4. *The energy transfer region:* We have chosen to study SRC in the $\omega$= 500-900 MeV energy transfer range. This is the kinematical region where the SRC contribution is significant compared to competing mechanisms, and both experimental requirements are satisfied and theoretical justification exists.

## The Target

1. *Experimentally:* $^3$He is clearly the optimum nucleus for to extract SRC, in a first, direct approach. It presents us with a kinematically complete experiment and reduced (or negligible) FSI.

2. *Theoretically:* $^3$He is the best understood (non-trivial) nucleus, with relativistically treated Faddeev equations providing exact solutions to discrete states and good approximations to the continuum. Its simplicity makes it possible to confidently estimate MEC and FSI effects.

# 6 Acknowledgments

Acknowledgments go to E. Jans, W. Hesselink, H. Blok, L. Lapikás and D. Groep, for fruitful discussions and for providing us with information on their recent NIKHEF experiments and on the properties of the HADRON3 device. We wish also to acknowledge the considerable theoretical assistance provided by W. Glöckle, J. Golak and J. Ryckebusch in terms of calculations (via our NIKHEF colleagues) and discussions. We wish to thank J.M. Laget, J.A. Tjon, R. Schiavilla, N. Isgur, and D. Walecka for their past comments and useful discussions on theoretical aspects of the proposal.

# Appendix A - Kinematics and Rates

The following is a description of Monte Carlo simulations that have been performed for the $^3$He(e, e′pp)n reaction in selected kinematics. The simulations have been performed with the program MCEEP.

MCEEP has been designed primarily for investigating $(e, e'p)$ reactions on light nuclei. As a result, it includes a large number of possibilities for the spectral functions of $^3$He. For this work, we have chosen the spectral function of Meier-Hajduk [43], and we have used the continuum region of the spectral function ($\epsilon_m > 2.2\ MeV$). At second-proton momenta of 300-390 MeV/c, the kinematics investigated here, we note that this spectral function describes the data quite well. In fact, for $^3$He, it is the only spectral function in MCEEP which contains both the two-body and three-body breakup information. The rates calculated are in PWIA, and assume that the cross section is described by

$$\sigma_{eeN} \sim K \sigma_{eN} S(\vec{p_r}, \epsilon_m). \tag{2}$$

Here, $\sigma_{eN}$ is the elementary electron-nucleon cross section, $K$ is a kinematical factor, and $S(\vec{p_r}, \epsilon_m)$ is the spectral function which gives the probability of finding a nucleon of momentum $\vec{p_r}$ and separation energy $\epsilon_m$.

## $^3$He(e, e′p)pn and $^3$He(e, e′pp)n Cross Sections in PWIA

Relating the eight-fold differential cross section for triple coincidences to the six-fold differential cross section for $(e, e'p)$ scattering to the continuum is considered below. For the $^3$He(e, e′p)pn reaction, the rate that one expects in an experiment is given by

$$\text{Doubles Rate}(Hz) = \left[ \frac{d^6\sigma}{d\Omega_e d\Omega_p dE_e dE_p} \times \Delta\Omega_e \Delta\Omega_p \Delta E_e \Delta E_p \right] N_t N_e \tag{3}$$

where the product $N_t N_e$ is the luminosity. The luminosity is expressed in terms of the target thickness and incident beam current (for the case of $^3$He) according to:

$$L = N_t N_e = 1.25 \times 10^{36} t(g/cm^2) I(\mu A) \tag{4}$$

Similarly, for the $^3$He(e, e′pp)n reaction, the experimental rate will be

$$\text{Triples Rate}(Hz) = \left[ \frac{d^8\sigma}{d\Omega_e d\Omega_{p1} d\Omega_{p2} dE_e dE_{p1}} \times \Delta\Omega_e \Delta\Omega_{p1} \Delta\Omega_{p2} \Delta E_e \Delta E_{p1} \right] N_t N_e \tag{5}$$

In the kinematics described here, the *total* momentum carried away by the $pn$ pair (in $(e, e'p)$ scattering) will be in the 300-390 MeV/c range at an angle of 180° to the three-momentum transfer vector. If we consider the entire momentum distribution, however, the angular distribution the second proton will be isotropic over $4\pi$ in the

centre-of-mass system of the $pn$ pair. This, of course, is true only in PWIA. Hence, we have the relationship that

$$\text{Triples Rate} = \text{Doubles Rate} \times f \tag{6}$$

where $f$ is the fraction of events where a second proton is detected in the Hadron3 detector. The details of how this fraction has been estimated is described in the following section.

Comparing Equations 3, 5, and 6, we see that

$$\frac{d^8\sigma}{d\Omega_e d\Omega_{p1} d\Omega_{p2} dE_e dE_{p1}} = \frac{d^6\sigma}{d\Omega_e d\Omega_p dE_e dE_p} \times \frac{f}{\Delta\Omega_{p2}} \tag{7}$$

It is precisely this relationship that allows us to relate the six-fold differential cross section estimates from MCEEP (in $(fm^2/MeV^2sr^2)$) to the eight-fold differential cross sections in PWIA (in $(fm^2/MeV^2sr^3)$) as calculated by the Bochum group and Laget.

## Determination of Second Proton Detection Fraction

The residual proton and neutron in the $^3$He(e, e′p)pn reaction must satisfy both momentum and energy conservation according to

$$\begin{aligned} \vec{\mathbf{p_2}} + \vec{\mathbf{p_n}} &= -\vec{\mathbf{p_R}} \\ E_2 + E_n &= \omega + M_T - E_{p_1}. \end{aligned} \tag{8}$$

All of the information on the right hand sides of the above equations is known from the electron and first proton kinematics. Hence, we may calculate directly then the invariant mass of the $(pn)$ pair, defined as

$$(m^*)^2 = (E_2 + E_n)^2 - (\vec{\mathbf{p_2}} + \vec{\mathbf{p_n}})^2. \tag{9}$$

The energies of the proton and neutron in the $(pn)$ centre-of-mass are given by

$$\begin{aligned} E_2^* &= \frac{m^*}{2} + \frac{(m_p^2 - m_n^2)}{2(m^*)^2} \\ E_n^* &= \frac{m^*}{2} - \frac{(m_p^2 - m_n^2)}{2(m^*)^2} \end{aligned} \tag{10}$$

The procedure for determining the fraction of protons which will be detected by Hadron3 (which is placed at -180° to $\vec{q}$) is as follows:

- The above equations are used to calculate the momenta of the proton and neutron in their centre-of-mass frame.
- We define an angle, $\theta_2^*$, of the proton. Hence, the neutron angle will be $\theta_n^* = \theta_2^* - 180°$.

- The angles and momenta of the proton and neutron *in the lab frame* are defined according to

$$\begin{aligned}
\tan(\theta_2) &= \frac{p_2^* \sin(\theta_2^*)}{\gamma_c(p_2^* \cos(\theta_2^*) + \beta_c E_2^*)} \\
\tan(\theta_n) &= \frac{p_n^* \sin(\theta_n^*)}{\gamma_c(p_n^* \cos(\theta_n^*) + \beta_c E_n^*)} \\
p_2 &= \frac{p_2^* \sin(\theta_2^*)}{\sin(\theta_2)} \\
p_n &= \frac{p_n^* \sin(\theta_n^*)}{\sin(\theta_n)}
\end{aligned} \tag{11}$$

  with $\gamma_c = (E_2 + E_n)/m^*$ and $\beta_c^2 = 1 - 1/\gamma^2$.

- According to Laget, in Phys. Rev. C35 (1987), 832, the eight-fold differential cross-section can be expressed:

$$\frac{d^8\sigma}{d\Omega_e d\Omega_{p1} d\Omega_{p2} dE_e dE_{p1}} = \Gamma_v \frac{E_n p_2^3 p_1^2}{E_1 |E_n \mathbf{p}_2^2 - E_2 \mathbf{p}_n \cdot \mathbf{p}_2|} \left[\frac{Q}{P}\right]_{cm} \frac{d^3\sigma}{(d\Omega_1)_{cm} d\mathbf{p}_n}, \tag{12}$$

  where $Q$ and $P$ are the proton total energy and momentum measured in the centre-of-mass frame of the two detected protons, and $\Gamma_v$ is the virtual photon flux defined according to

$$\Gamma_v = \frac{\alpha}{2\pi^2} \left(\frac{E'}{E}\right) \left(\frac{q}{1-\epsilon}\right) \frac{1}{Q^2}. \tag{13}$$

The reduced cross section in the above equation is the product of the momentum distribution of the spectator neutron and the cross-section of the disintegration of the $pp$-pair. Hence, we expect it to be essentially constant for a given set of electron and detected first proton kinematics, since defining these also defines the neutron and second proton momenta as well. While the virtual photon flux depends only on the electron kinematics, the kinematic factor in the above equation also depends on the momenta of all three hadrons in the final state. Using Equations 12 and 13, together with the published cross sections of Laget, we have calculated the eight-fold differential cross section as a function of $\theta_2$, the angle of the second proton (with respect to $-\vec{q}$) in the lab frame. From this distribution, we can calculate the fraction of second protons, $f$, that will be detected in Hadron3. The fraction of detected protons for recoil momenta in the range of 300-450 MeV/c is about 11%.

## Detector Acceptance Issues

The second-proton momentum range that we have chosen falls entirely within the third-arm detector acceptance. This is shown in Figure 5. Here, the solid curve is the momentum phase space acceptance of Hadron3 as specified in the three-body kinematics phase space Monte Carlo program, AEE2XB [44]. We also note that the low momentum limit in the AEE2XB calculation (which corresponds to an energy of 45 MeV) takes into account the energy losses in the $^3$He target, the windows of the scattering chamber, and in the Hadron3 detector itself.

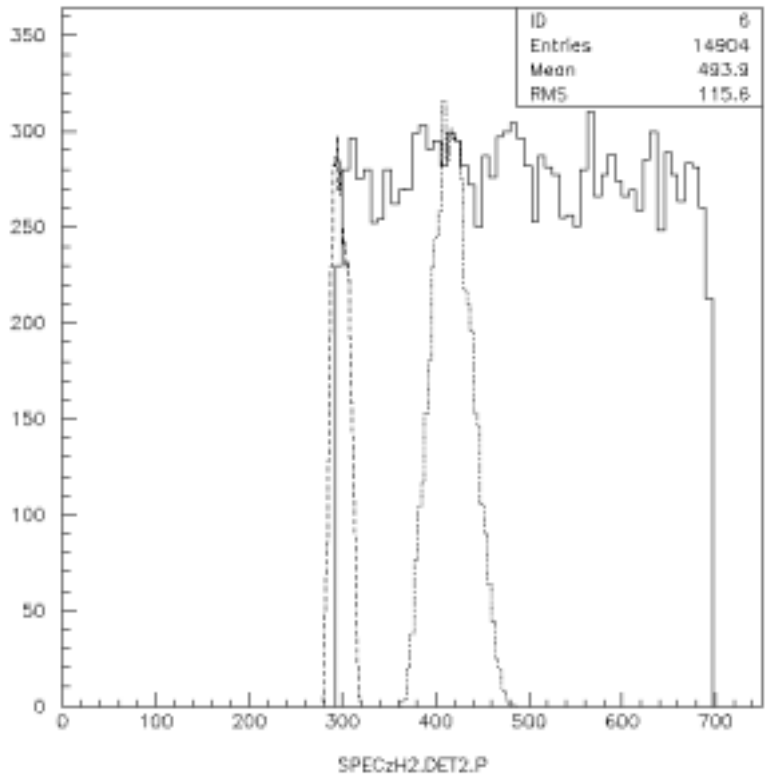


Figure 5: Momentum Distributions of the Second Proton in the $^3$He(e, e′pp)n reaction. The solid curve is the phase space prediction of AEE2XB. The dashed curve is the case of zero neutron momentum corresponding to a second-proton momentum of 300 MeV/c. The dotted curve is the zero neutron momentum case which corresponds to a second-proton momentum of 420 MeV/c. These two curves bracket the range of interest in this proposal.

# Appendix B - Comparison to Other Approaches

SRC constitute a small component of total two-nucleon emission cross section and this fact necessitates the three driving experimental specifications of this proposal: the L/T separation (to isolate one-body currents driven by SRC from that of MEC and IC driven two-body currents); the super-parallel kinematics (to isolate one-body currents and to suppress rescattering in the pp channel); and, finally, the high luminosity ($4\times10^{37}$ cm$^{-2}$s$^{-1}$) needed to extract the small cross sections.

*There is no approved program at JLab to pursue SRC with the method outlined here.* The relationship of our proposal to the approved two-nucleon emission program with CLAS in Hall B and to an alternate attempt to probe SRC in Hall C, is explained below. We consider the three approaches to be complementary.

Hall B Correlation Studies

There is an approved experiment to investigate the $^3$He(e, e′pp)X reaction using the CLAS detector in Hall B (E89-031). The specific goal of that experiment is a survey of the two-nucleon knockout reaction on selected nuclei, and it does not overlap with the selective scientific goals of our proposed experiment in Hall A. The large solid angle acceptance of CLAS covers phase space which is of no direct interest to SRC. The issues of the L/T separation and luminosity further establish this experiment as different in nature, goals, and methodology, and thus render it complementary, rather than similar, to ours. However, final comparisons of total cross sections, on selected processes of overlap, will add confidence to the conclusions of this experiment.

A(e, e′pN) Reactions in the $x_{Bj} > 1$ Region

An experiment in Hall C (E97-106) has been approved to search for two-nucleon correlations using the (e, e′pN) reaction in nuclei. This experiment will probe *the momentum of the proton before the interaction.* The authors of this experiment have advocated the choice of a high Q$^2$ and $x_{Bj} > 1$ kinematic regime for the experiment, where FSI are minimized. Interestingly, such kinematics probe a similar region of relative nucleon momenta (300-500 $MeV/c$), and hence similar $N$-$N$ separation distances, as in this proposal, and access primarily 2BC. In contrast, however, we have chosen smaller $x_{Bj}$ and Q$^2$, where the experimental rates will be comparatively much larger. The main difference between the two approaches is the level of model-dependency in the extraction of the SRC component. E97-106 will have to rely heavily on theoretical modelling, whereas our method is much less model dependent, due to the larger suppression of competing mechanisms. Nevertheless, valuable information on the MEC and IC channels should become available from E97-106, and as such, the physics of the two approaches is complementary.

# References


[1] Workshop on the Short-Range Structure in Nuclei, Jefferson Lab, March 15-16, 1996.

[2] Hall A Few-Body Working Group Meeting, Jefferson Lab, November 6-8, 1997.

[3] $10^{th}$ NIKHEF Mini-Conference on "Studies of Few-Body Systems with High Duty-Factor Electron Beams", NIKHEF, January 6-7, 1999.

[4] S. Auffret *et al.*, Phys. Rev. Lett. **55** (1985) 1362.

[5] T. Emura *et al.*, Phys. Rev. **C49** (1994) R597.

[6] T. Emura *et al.*, Phys. Rev. Lett. **73** (1994) 404.

[7] C. Marchand *et al.*, Phys. Rev. Lett. **60** (1988) 1703.

[8] Th.S. Bauer, Nucl. Phys. **A546** (1992) 181c.

[9] Hall A Few-Body Working Group Meeting, Jefferson Lab, May 23, 1999.

[10] J.M. Laget, Phys. Rev. **C35** (1987) 832.

[11] J. Ryckebusch, Laboratory for Nuclear Physics, University of Gent, Internal Report SSF95-12-01.
J. Ryckebusch, "Workshop on Electron Nucleus Scattering", Elba International Physics Center, July 1-5, 1996.

[12] S. Boffi, Proceedings of the Topical Workshop on Two Nucleon Emission, ed. O. Benhar and A. Fabrocini (ETS editrice, Pisa, 1991) 87.

[13] C. Giusti *et al.*, Nucl. Phys. **A546** (1992) 607.

[14] J. Ryckebusch, Phys. Lett. **B383** (1996) 1.

[15] W. Geurts *et al.*, Phys. Rec. **C54** (1996) 1144.

[16] V.D. Efros *et al.*, Phys. Rev. **C58** (1998) 582.

[17] S. Dumalski *et al.*, Phys. Rev. **C**, in preparation.

[18] J.A. Tjon, J.M. Laget, J. Ryckebusch, S. Jeschonnek, private communication.

[19] H. Arenhovel and M. Sanzone, Few Body Systems Suppl. 3, Springer Verlag, Wien, N.Y.

[20] P. Weber *et al.*, Nucl. Phys. **A534** (1991) 541.

[21] A. Lehmann *et al.*, Phys. Rev. **C55** (1997) 2931; A. Lehmann *et al.*, PSI-PR-97-16 (June 1997).

[22] G.M. Huber *et al.*, Nucl. Phys. **A624** (1997) 623.

[23] E. van Meijgaard and J.A. Tjon, Phys. Rev. **45** (1992) 1463.

[24] J. Golak *et al.*, Phys. Rev. **C51** (1995) 1638.

[25] S. Jeschonnek and T.W. Donnelly, Phys. Rev. **C59** (1999) 2676.

[26] G.J. Lolos *et al.*, Phys. Rev. Lett. **80** (1998) 241;
G.M. Huber, G.J. Lolos and Z. Papandreou, Phys. Rev. Lett. **80**, 5285 (1998);
Z. Papandreou, G.M. Huber, G.J. Lolos, E.J. Brash, and B.K. Jennings, Phys. Rev. **C59** (1999) R1864;
M. Kagarlis *et al.*, Phys. Rev. **C**, in press.

[27] G.J. Lolos *et al.*, E99-101, submitted to PAC-16.

[28] W.J. Kasdorp, Ph.D. Thesis, University of Utrecht (1997); Few-Body Systems, in press.

[29] J.J. van Leeuwe, Ph.D. Thesis, University of Utrecht (1996); submitted to Phys. Rev. Lett.

[30] L.J.H.M. Kester *et al.*, Phys. Rev. Lett. **74** (1995) 1712.

[31] G.J.G. Onderwater *et al.*, Phys. Rev. Lett. **78** (1997) 4893.

[32] G.J.G. Onderwater *et al.*, Phys. Rev. Lett. **81** (1998) 2213.

[33] W.H.A. Hesselink *et al.*, *Probing Short-Range Correlations in* $^3$He *and* $^{16}$O *using the reaction* $(e,e'pp)$, Proceedings of the $10^{th}$ NIKHEF Mini-Conference, January 5-7, 1999.

[34] D. Groep *et al.*, Proceedings of the International Nuclear Physics Conference INPC, Paris 1998, to appear as a supplement to Nucl. Phys. A.

[35] R. Starink, Ph.D. Thesis, Free University of Amsterdam, 1999, unpublished.

[36] C. Giusti *et al.*, Phys. Rev. **C57** (1998) 1691.

[37] C. Giusti and F.D. Pacati, Nucl. Phys. **A535** (1991) 573.

[38] M.J. Dekker *et al.*, Phys. Lett. **289B** (1992) 255.

[39] J.M. Laget, private communication.

[40] W.H.A. Hesselink, "Workshop on Electron Nucleus Scattering", Elba International Physics Center, July 1-5, 1996.

[41] D.J.J. de Lange *et al.*, Nucl. Instr. Meth. in Phys. Res. **A406** (1998) 182; *ibid.*, **A412** (1998) 254.
K. de Jager, private communication.

[42] J.A. Tjon, private communication.

[43] H. Meier-Hajduk *et al.*, Nucl. Phys. **A449** (1983) 332.

[44] E. Offermann, private communication.